Inorg. Chem. **2008**, *47*, 5685−5695

Novel Chelate Ring-Opening Induced by Silver(I) of Five-Coordinate Palladium(II) and Platinum(II) Complexes Containing Tripodal Polyphosphines

D. Fernández-Anca, M. Inés García-Seijo, Alfonso Castiñeiras, and M. Esther García-Fernández*

Departamento de Química Inorgánica, Universidad de Santiago de Compostela, E-15782 Santiago de Compostela, Spain

Received December 14, 2007

The ionic complexes $[Pd(NP_3)X]X$ [NP_3 = tris[2-(diphenylphosphino)ethyl]amine, X = Cl (**1**), Br(**2**)] and $[M(PP_3)X]X$ [PP_3 = tris[2-(diphenylphosphino)ethyl]phosphine, M = Pd, X = Cl (**3**), Br(**4**); M = Pt, X = Cl (**5**), Br (**6**)] contain square pyramidal (**1**, **2**) and trigonal bipyramidal (**3**−**6**) cations with three fused chelate rings to M and one M−X bond. By addition of AgX salts (X = Cl, Br, NO_3) an unexpected ring-opening reaction occurs with formation of the heteronuclear species $PdAg(NP_3)X_3$ [X = Cl (**7**), Br (**8**)], $MAg(PP_3)X_3$ [M = Pd, X = Cl (**9**), Br (**10**), NO_3 (**13**); M = Pt, *X* = Cl (**11**), Br (**12**), NO_3 (**14**)]. The complexes have been characterized in the solid state and solution. The X-ray crystal structures of **9** and **13** reveal a distorted square-planar arrangement to Pd(II) that is coordinated to three P of PP_3 (the central and two terminal atoms) and to one chloride (**9**) or one oxygen atom of NO_3 (**13**). The resultant dangling phosphorus of the ring opening is bound to Ag(I) that completes the three- [$PAgCl_2$ (**9**)] and four-coordination [$PAg(ONO_2)(O_2NO)$ (**13**)] through the donor atoms of the anions with the nitrates in **13** unusually acting as both mono- and bidentate ligands. Complexes **7**, **8**, **10**, and **11** undergo oligomerization in solution. Complex **10** oligomerizes giving rise to the ionic compound $[Pd_4Ag_2(PP_3)_2\ Br_9]Br$ (**10a**) whose X-ray crystal structure indicates the presence of cations with a $Pd(\mu\text{-}Br)_3Pd$ unit that connects via bromide bridges two $BrPdP_2PPAg\ Br_2$ fragments containing distorted square-planar and trigonal-planar Pd(II) and Ag(I) centers, respectively. The palladium(II) metal centers in the central unit afford the five-coordination ($PdBr_5$) with a distorted trigonal bipyramidal geometry. The ionic system $[Pt_2Ag_2(PP_3)_2\ Cl_5]Cl$ (**11a**) consists of chloride anions and heteronuclear monocations. The X-ray crystal structure reveals that the cations contain two distorted square-planar $ClPtP_3$ units bridged by one $PAgCl(\mu\text{-}Cl)_2AgP$ fragment that is bearing tetrahedral ($PAgCl_3$) and trigonal planar $PAgCl_2$ silver(I) centers. Further additions of the corresponding AgX salts to complexes **7**−**14** did not give rise to any new ring-opening reaction.

Introduction

Studies on heterometallic systems are of particular current interest because of the wide variety of applications as catalysts, semiconductors, optical devices, and pharmaceutical agents offering prospects for advantageous synergistic effects where the reactivity of the whole can be greater than the sum of the parts.[1,2] Complexes supported by sulfide,[3] chloride,[4] carboxylate,[5] pyrazolate,[6] alkoxysilyl,[7] and diphos-

* To whom correspondence should be addressed. E-mail: qiegfq@usc.es. Phone: 34-981-563100/14241. Fax: 34-981-597525.

(1) (a) Wheatley, N.; Kalck, P. *Chem. Rev.* **1999**, *99*, 3379. (b) Stephan, D. W.; Nadasdi, T. T. *Coord. Chem. Rev.* **1996**, *147*, 147. (c) Bullock, R. M.; Casey, C. P. *Acc. Chem. Res.* **1987**, *20*, 167. (d) Stephan, D. W. *Coord. Chem. Rev.* **1989**, *95*, 41. (e) Adams, R. D. In: *Comprenhensive Organometallic Chemistry II*; Wilkinson, G., Stone, F. G. A., Abel, E. W. Eds.; Pergamon: Oxford, U. K., 1995; Vol. *10*, p 1. (f) Cheng, C.-C.; Pai, C.-H. *J. Inorg. Biochem.* **1998**, *71*, 109. (g) Sevillano, P.; Habtemariam, A.; Parsons, S.; Castiñeiras, A.; García, M. E.; Sadler, P. J. *J. Chem. Soc., Dalton Trans.* **1999**, 2861. (h) Sevillano, P.; Habtemariam, A.; García-Seijo, M. I.; Castiñeiras, A.; Parsons, S.; García, M. E.; Sadler, P. J. *Aust. J. Chem.* **2000**, *53*, 635.

(2) (a) Bosnich, B. *Inorg. Chem.* **1999**, *38*, 2554. (b) Watkins, S. E.; Craig, D. C.; Colbran, S. B. *J. Chem. Soc., Dalton Trans.* **2002**, 2423. (c) Hettiarachchi, S. R.; Schaefer, B. K.; Yson, R. L.; Staples, R. J.; Herbst-Irmer, R.; Patterson, H. H. *Inorg. Chem.* **2007**, *46*, 6997. (d) Colis, J. C. F.; Staples, R.; Tripp, C.; Labrecque, D.; Patterson, H. H. *J. Phys. Chem. B* **2005**, *109*, 102. (e) Colis, J. C. F.; Larochelle, C.; Fernández, E. J.; López-de-; Luzuriaga, J. M.; Monge, M.; Laguna, A.; Tripp, C.; Patterson, H. H. *J. Phys. Chem. B* **2005**, *109*, 4317. (f) Colis, J. C. F.; Larochelle, C.; Staples, R.; Herbst-Irmer, R.; Patterson, H. H. *Dalton Trans.* **2005**, 675.

(3) Fong, S.-W. A.; Yap, W. T.; Vittal, J. J.; Henderson, W.; Hor, T. S. A. *J. Chem. Soc., Dalton Trans.* **2002**, 1826.

10.1021/ic702419r CCC: $40.75
Published on Web 05/29/2008

Scheme 1. Reactions of **1**−**6** with AgX (X = Cl, Br) to Form the Heteronuclear Complexes **7**−**12**

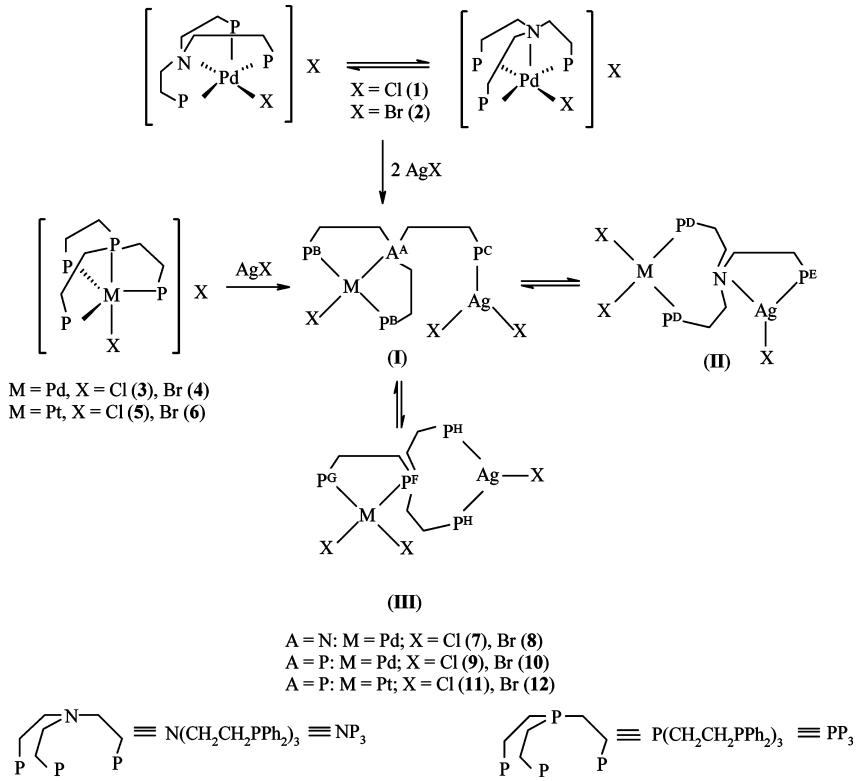

phine[8] ligands or closely related derivatives[9] have been shown to be very useful metalloligands for the synthesis of a vast diversity of homo and heterometallic aggregrates.

Although a variety of heterobimetallic d^0-d^8, d^6-d^8 and d^8-d^{10} centers has been studied by utilizing diphosphines (dppm = $Ph_2PCH_2PPh_2$, dppa = $Ph_2PNHPPh_2$, dmpe = $Me_2P(CH_2)_2PMe_2$)[10–14a] the arrangement of several metal centers assembling tri- or tetraphosphine ligands is more uncommon.[14b,15] Tanase[15a] et al. have reported that the reaction of $[Pt_2(XylNC)_6](PF_6)_2$ (Xyl = 2,6-dimethylphenyl) with the linear triphosphine ligand bis-[(diphenylphosphino)methyl]phenylphosphine (dpmp) afforded a mixture of isomeric diplatinum complexes, *syn*- and *anti*- $[Pt_2(\mu\text{-dpmp})_2(XylNC)_2](PF_6)_2$ that are good precursors of homo- and heterometallic small size clusters because they have uncoordinated phosphine units. Thus, the reaction of the *syn*-complex with d^{10} Pt and Pd fragments gives linearly ordered LPtPtML structures (L = Xyl); however, with monovalent group 11 metal ions (d^{10} configuration) it results in Y-shaped $LPt_2M'L$ (M′ = Ag, Au) or rhombic LPt_2CuXL (X = Cl, Br, I) structures. It should be noted that despite the superficially similar monovalent cations Au(I) and Ag(I) both displaying similar strucutural motifs, as we have just mentioned, there are some marked differences in phosphine coordination within the group 11 series of [M′(TP)Cl] and [M′XPR$_3$] (M′ = Ag, Au; TP = bis[2-(diphenylphosphino)phenyl]phenylphosphine; X = Cl, Br) compounds. The crystal structures of complexes containing the TP ligand[15b] indicate a preference for coordination number two over three for gold in contrast to silver. In parallel, the gold compounds with linear $XAuPR_3$ entities prefer to interact via close Au···Au contacts keeping the linear structure approximately intact, while the corresponding silver (or copper)

(4) (a) López, G.; García, G.; Sánchez, G.; de Haro, C.; Santana, M. D.; Casabó, J.; Caldes, M.; Mejías, M.; Molins, E.; Miratvilles, C. *J. Chem. Soc., Dalton Trans.* **1991**, 3311. (b) Polborn, K.; Severin, K. *Eur. J. Inorg. Chem.* **1998**, 1187. (c) Chesnut, D. J.; Haushalter, R. C.; Zubieta, J. *Inorg. Chim. Acta* **1999**, *292*, 41. (d) Öhm, M.; Schulz, A.; Severin, K. *Eur. J. Inorg. Chem.* **2000**, 2623. (e) Ara, I.; Berenguer, J. R.; Eguizábal, E.; Forniés, J.; Lalinde, E.; Martín, A. *Eur. J. Inorg. Chem.* **2001**, 1631.

(5) (a) Tan, A. L.; Low, P. M. N.; Zhou, Z.; Zheng, W.; Wu, B.; Mak, T. C. W.; Hor, T. S. A. *J. Chem. Soc., Dalton Trans.* **1996**, 2207. (b) Neo, Y. C.; Vittal, J. J.; Hor, T. S. *J. Chem. Soc., Dalton Trans.* **2002**, 337.

(6) Fackler, J. P., Jr.; Raptis, R. G.; Murray, H. H. *Inorg. Chim. Acta* **1992**, *193*, 173.

(7) Blin, J.; Braunstein, P.; Fisher, J.; Kickelbick, G.; Knorr, M.; Morise, X.; Wirth, T. *Inorg. Chem.* **1999**, *13*, 2159.

(8) Hutton, A. T.; Pringle, P. G.; Shaw, B. L. *Inorg. Chem.* **1985**, *8*, 1677.

(9) (a) Fornies-Camer, J.; Masdeu-Bulto, A. M.; Claver, C.; Tejel, C.; Ciriano, M. A.; Cardin, Ch. J. *Organometallics* **2002**, *21*, 2609. (b) Al-Jibori, S. A.; Amin, O. H.; Al-Allaf, T. A. K.; Davis, R. *Transition Met. Chem.* **2001**, *26*, 186.

(10) Matare, G. J.; Tess, M. E.; Yang, Y.; Abboud, K. A.; McElwee-White, L. *Organometallics* **2002**, *21*, 711.

(11) Braunstein, P.; Durand, J.; Morise, X.; Tiripicchio, A.; Ugozzoli, F. *Organometallics* **2000**, *19*, 444.

(12) Yip, H. K.; Lin, H. M.; Wang, Y.; Che, C. M. *Inorg. Chem.* **1993**, *32*, 3402.

(13) Carr, S. W.; Pringle, P. G.; Shaw, B. L. *J. Organomet. Chem.* **1988**, *341*, 543.

(14) (a) Butts, M. D.; Bergman, R. G. *Organometallics* **1994**, *13*, 1899. (b) Aizawa, S.; Saito, K.; Kawamoto, T.; Matsumoto, E. *Inorg. Chem.* **2006**, *45*, 4859.

(15) (a) Tanase, T.; Toda, H.; Yamamoto, Y. *Inorg. Chem.* **1997**, *36*, 1571. (b) Zank, J.; Schier, A.; Schmidbaur, H. *J. Chem. Soc., Dalton Trans.* **1999**, 415. (c) Schwerdfeger, P.; Hermann, H. L.; Schmidbaur, H. *Inorg. Chem.* **2003**, *42*, 1334. (d) Bauer, A.; Schmidbaur, H. *J. Am. Chem. Soc.* **1996**, *118*, 5324.

Scheme 2. Structures for Oligomers **7a**, **8a**, **10a**, and **11a**

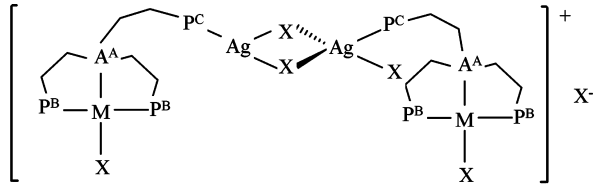

A = N: M = Pd, X = Cl (**7a**), Br (**8a**)
A = P: M = Pt, X = Cl (**11a**)

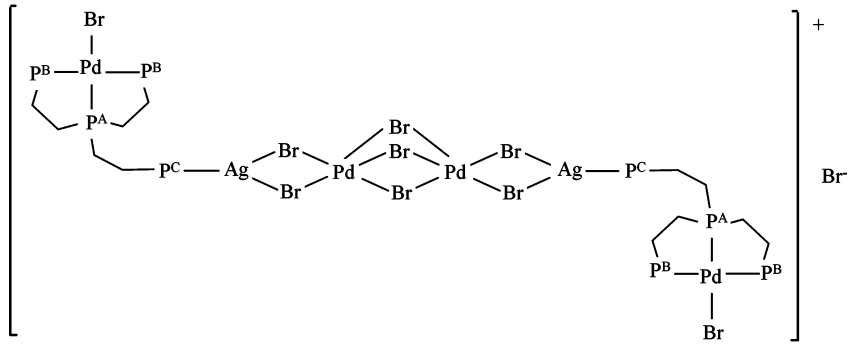

10a

Scheme 3. Ring-Opening Reaction of $[M(PP_3)Cl]Cl$ (M = Pd, Pt) Induced by $AgNO_3$ versus the Chloro Substitution Reaction of [M(triphos)Cl]Cl (triphos = $PhP(CH_2CH_2PPh_2)_2$) by Nitrate

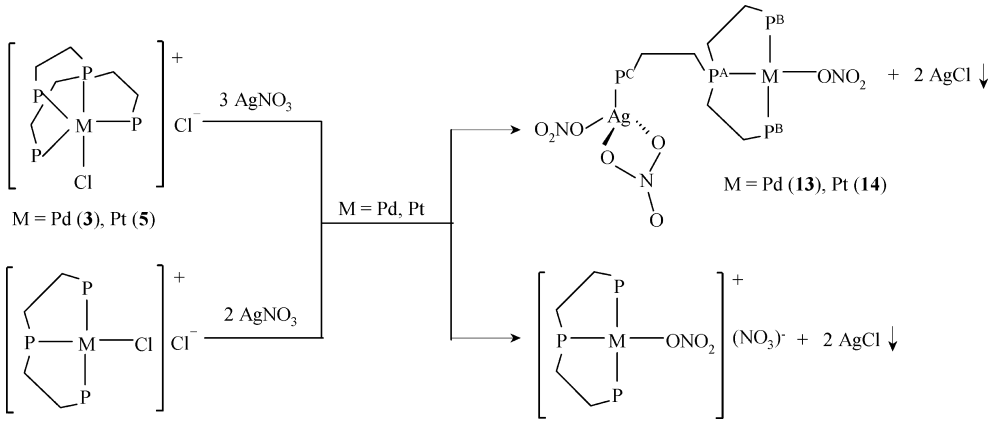

compounds oligomerize with PR_3 ligands attached to M_2X_2 units containing bridging ligands X where each metal atom achieves the formal coordination number of three.[15c]

In previous studies[1h,16,17] on the reactivity of the square-planar complexes [M(triphos)Cl]Cl (M= Pd, Pt; triphos = bis[2-(diphenylphosphino)ethyl]phenylphosphine) with copper(I), silver(I), and gold(I) salts we confirmed significant differences between gold(I) and the lighter group 11 monocations. The reaction with $AgNO_3$ leads to the formation of $[M(triphos)(ONO_2)](NO_3)$ whose X-ray crystal structure constitutes an unusual example of complex containing Pd-ONO_2 bonds.[16] The cationic square-planar complexes are not altered by addition of AgCl, and by interaction with CuCl, the formation of dichlorocuprate(I) counteranions was confirmed in the solid state and solution.[17a] In contrast, the two square-planar compounds react with Au(tdg)X (tdg = thiodiglycol; X = Cl, Br) via a ring opening process to form the neutral heterobimetallic systems $MAu(tripos)X_3$ containing square-planar and linear arrangements for M and Au, respectively.[16,1h] On the other hand, the addition of one equivalent of Au(tdg)Cl or CuCl to the trigonal bipyramidal compounds $[M(PP_3)Cl]Cl$ results, via a ring-opening reaction, in the formation of heterobimetallic compounds of the type $[MAu(PP_3)Cl_2]Cl$ or $MCu(PP_3)Cl_3$ containing distorted square-planar and linear or trigonal planar, M(II) and Au(I) or Cu(I) centers, respectively.[17] A second ring-opening process occurs by addition of another equivalent of Au(tdg)Cl affording $MAu_2(PP_3)Cl_4$ while the second equivalent of CuCl leads to $[MCu(PP_3)Cl_2](CuCl_2)$.

(16) (a) Fernández, D.; Sevillano, P.; García-Seijo, M. I.; Castiñeiras, A.; Jánosi, L.; Berente, Z.; Kollár, L.; García-Fernández, M. E. *Inorg. Chim. Acta* **2001**, *312*, 40. (b) Umemoto, K.; Tsukui, H.; Kusukawa, T.; Biradha, K.; Fujita, M. *Angew. Chem., Int. Ed.* **2001**, *40*, 2620.

(17) (a) Fernández, D.; García-Seijo, M.; Sevillano, P.; Castiñeiras, A.; García-Fernández, M. E. *Inorg. Chim. Acta* **2005**, *358*, 2575. (b) Fernández, D.; García-Seijo, M. I.; Castiñeiras, A.; García-Fernández, M. E. *Dalton Trans.* **2004**, 2526.

Table 1. Conductivities, Mass Spectra, and Far Infrared Data for Compounds **7**−**14**

compound	Λ(DMF/$CH_3CN^{\blacklozenge}$) (Ω^{-1} cm^2 mol^{-1})	MS(L-SIMS) *m/z* (% abundance)	IR[a] (M−X)/(Ag−X)*/(N−O) ν_{max} /cm^{-1}
7	101.9$^{\blacklozenge}$	1907 (5%)[b], 936(5%)[c] 794 (57%)[d]	300m, 215vs*, 210sh*, 190sh*
8·Et_2O	101.9$^{\blacklozenge}$	1024 (2%)[c], 838 (3%)[d]	252vs, 248vs, 150vs*, 140vs*
(**9**)·$2H_2O$	28.3	955 (3%)[c], 920 (2%)[e], 811 (62%)[d]	309s, 282s, 175sh*
(**10**)·$4H_2O$	28.2	1994 (2%)[f], 1041(3%)[c], 776(5%)[g]	255m, 250m, 232m, 146vs*, 136vs*
11	29.7	2088 (3%)[h], 1044 (3%)[c]	309vs, 170m*, 155m*, 145m*
(**12**)·$0.5Et_2O$	24.2	945(1%)[i]	262m, 255m, 142s*, 130s*
(**13**)·$2H_2O$·$0.5Et_2O$	165.7	1009 (2%)[c], 855 (2%)[j], 776 (2%)[g]	1480s, 1434s, 1384s, 1275s
(**14**)·$2H_2O$·Et_2O	186.4	1098 (2%)[c], 974 (4%)[j], 865 (46%)[g]	1482w, 1434m, 1384vs, 1275w

[a] (M= Pd, Pt; X = Cl, Br); L: NP_3 = $N(CH_2CH_2PPh_2)_3$, PP_3 = $P(CH_2CH_2PPh_2)_3$. [b] ($M_2Ag_2L_2X_5$). [c] ($MAgLX_2$). [d] (MLX). [e] (MAgLX). [f] [M_4Ag_2(L-4 $Ph)_2X_8$]. [g] (ML). [h] ($M_2Ag_2L_2X_4$). [i] [MAg(L-PPh_2)X_2]. [j] (MAgL).

Table 2. $^{31}P\{^1H\}$ NMR Data at Room Temperature for Complexes **7**−**14**

compound[a]	$\delta P^A/P^F$	δP^B	$\delta P^D/P^H$	δP^C	$\delta P^E/P^G$	$^1J(^{31}P,^{195}Pt)$	$^1J(^{31}P^H,\ ^{107/109}Ag)/^3J(^{31}P^A,^{31}P^C)$	solvent
7		31.5s	11.8s	−17.6br	−11.6br			$CDCl_3$
7(213 K)		34.0br, 33.0s	13.7s	−7.3br, −9.0br	−4.6br			CD_2Cl_2
8		44.5s, 37.7br	15.0s	−3.9s, −4.6br	−11.6br			CD_3OD+DMSO-d_6
9	118.2s	42.0br		42.0br				$CDCl_3$
9(203 K)	115.0br/93.0br	47.3s	2.1br	2.1br	72.0s		400 av.	CD_2Cl_2
10a[b]	125.9s	40.1br		40.1br				DMSO-d_6
11[c]	90.1d	44.4d	32.0br	32.0br	11.0d	2898/2495/3590	49	$CDCl_3$
11 (203 K)	88.0br/11.6br	43.6s, 42.3s	1.0br	1.0br	11.6br	2948/2494,2484/3687	455 av.	CD_2Cl_2
12	114.0br	27.8br		27.8br				$CDCl_3$
13	119.0d	49.8s		10.4d			62	$CDCl_3$
14[c]	79.3d	46.1s		9.7d		3146/2616		$CDCl_3$

[a] See Schemes 1, 2, and 3 for labels in P atoms. The underlined broad signals include two or more types of P atoms. [b] **10** in DMSO-d_6 = **10a** + $Ag(PP_3)Br$. The broad signal at δ 40.1 includes P^B and P^C of **10a** and the resonances due to $Ag(PP_3)Br$. [c] $\delta(^{195}Pt)$ for **11** and **14** in $CDCl_3/^1J(^{195}Pt,^{31}P)$: (**11**) −4420 dd, −4818 dt/ 3642, 2944, and 2471. (**14**) −4680 dt/ 3096, 2633.

Owing to the limited studies on the formation of heterobimetallic complexes containing silver(I) and tripodal polyphosphine ligands,[18] this work deals with the synthesis and characterization of new mixed metal compounds afforded by interaction between AgX salts (X = Cl, Br, NO_3) and the five-coordinate precursors [M(L)X]X (M = Pd, Pt; L = NP_3, PP_3; X = Cl, Br).

Results and Discussion

Syntheses. Schemes 1 and 2 show the halo complexes prepared in this work. Compounds **9**−**12** were afforded by addition of AgX to **3**−**6** in a 1:1 ratio while complexes **7** and **8** were prepared using a 1:2 precursor to silver ratio with subsequent removal of excess AgX by filtration. The interaction between **1** or **2** and one equivalent of AgX yields solids which we were not able to identify unambiguously but which most likely correspond to mixtures of heteronuclear isomers coexisting with unreacted precursors. The nitrate derivatives **13** and **14** (Scheme 3) were prepared using a 1:3 Pd(II)/Pt(II) to $AgNO_3$ ratio.

The precursors **1**−**6** were previously reported.[17b] The heteronuclear systems **7** and **11** exhibited yellow colors while **9** and **10** were prepared as pink hydrates, **8** and **12** as yellow ether solvates, and **13** and **14** both as beige hydrate and etherate species. Colorless crystals of **10a/13** were prepared by adding AgBr(as solid)/$AgNO_3$(in solution) to solutions of (**4**)·$2H_2O$/(**3**)·$4H_2O$, while colorless single crystals of **9** and **11a** were obtained as (**9**)·CH_3OH·$2H_2O$ and **11a**·$CHCl_3$·H_2O starting from solutions of (**9**)·$2H_2O$ and **11**, respectively (vide infra).

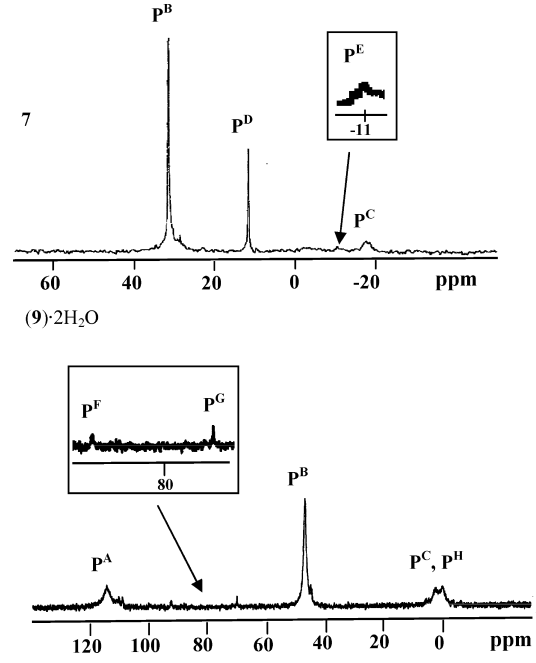

Figure 1. $^{31}P\{^1H\}$ NMR spectra for **7** (r.t., $CDCl_3$) and (**9**)·$2H_2O$ (203 K, CD_2Cl_2).

The mixed metal complexes afforded in 61−97% yields showed higher solubilities for Pd(II) than for Pt(II), and all of them were soluble in dimethylformamide and dimethylsulfoxide.

Characterization. The heteronuclear compounds **7**−**14** were characterized by conductivity measurements, L-SIMS mass spectra, far-infrared, ^{195}Pt and $^{31}P\{^1H\}$NMR spec-

(18) García-Seijo, M. I.; Habtemariam, A.; Fernández-Anca, D.; Parsons, S.; García-Fernández, M. E. *Z. Anorg. Allg. Chem.* **2002**, *628*, 1075.

(19) Fernández, D.; García-Seijo, M. I.; Kégl, T.; Petócz, G.; Kollár, L.; García- Fernández, M. E. *Inorg. Chem.* **2002**, *47*, 4435.

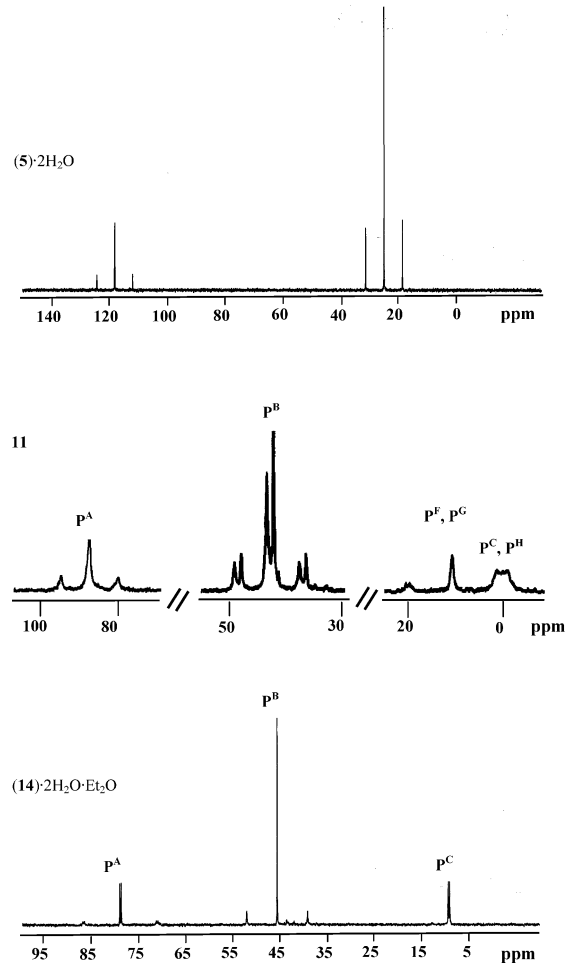

Figure 2. ^{31}P $\{^1H\}$ NMR spectra for (**5**)·$2H_2O$ (r.t., $CDCl_3$), **11** (203 K, CD_2Cl_2) and (**14**)·$2H_2O$·Et_2O (r.t., $CDCl_3$).

troscopies (Tables 1 and 2 and Figures 1 and 2 and Supporting Information, Figures S1−S3), and **9**, **10a**, **11a**, and **13** were also characterized by X-ray diffraction (Tables 3–6 and Figures 3–5).

Complexes Containing Chlorides and Bromides As Coligands. In this section the characterization of compounds **7**−**12** is reported. Table 1 shows their conductivities, mass spectra, and far-infrared data. Attempts to prepare heteronuclear systems by interaction between $[Pt(NP_3)X]X$ and AgX (X = Cl, Br) were unsuccessful. All compounds show a neutral behavior in solution although for **7** and **8** the conductivities are in the higher limit for a non electrolyte in acetonitrile. The mass spectra show in all cases peaks due to heteronuclear fragments, and for **7**, **10**, and **11** there appear peaks assigned to $Pd_2Ag_2(NP_3)_2Cl_5$, $Pd_4Ag_2(PP_3\text{-}4Ph)_2Br_8$, and $Pt_2Ag_2(PP_3)_2Cl_4$ moieties, respectively, indicating the existence as oligomeric systems.

The bands observed in the far-infrared spectra are in agreement with the presence in the solids of bridging and/or terminal metal-halide bonds.[17b,20]

$^{31}P\{^1H\}$NMR Spectra For NP_3 Derivatives. The $^{31}P\{^1H\}$-NMR spectrum of **7** in $CDCl_3$ at room temperature shows four signals as observed in Figure 1. The broad singlets at δ 31.5 and 11.8 are assigned to phosphorus atoms bound to Pd(II) while the broad resonances at δ −11.6 and −17.6 are attributable to phosphorus bound to silver(I). Given the tendency of silver to undergo oligomerization via Ag(μ-$X)_2$Ag bridges (vide supra) and according to the L-SIMS data it seems that complex **7** exists in solution as a mixture of oligomers, one afforded by combination of monomers **I** and **II** (Scheme 1) and the other one by dimerization of monomer **I** (oligomer **7a**, Scheme 2). The resonance at lower field would correspond to phosphorus P^B mutually trans in monomer **I** and oligomer **7a**, and the resonance at δ 11.8 to phosphorus P^D trans to Cl in monomer **II**. When this spectrum is recorded at 213 K in CD_2Cl_2, the signals at δ 31.5 and −17.6 split into two resonances (Supporting Information, Figure S1, Table 2) allowing us to distinguish the different sets of phosphorus atoms P^B mutually trans bound to Pd(II) and phosphorus P^c bound to Ag(I) in oligomer **7a** ($4P^B + 2P^C$) and monomer **I** ($2P^B + 1\ P^C$). Similar results were found for complex **8** in CD_3OD/DMSO-d_6 at room temperature (Table 2).

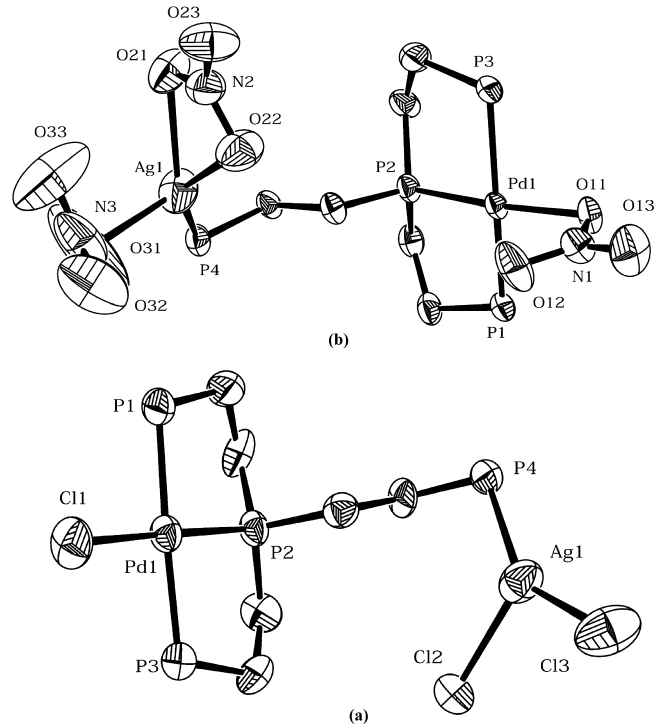

Figure 3. ORTEP diagram for **9** (a) and **13** (b). Phenyl rings omitted for clarity.

$^{31}P\{^1H\}$NMR Spectra for PP_3 Derivatives. This section describes the characterization in solution of compounds $PdAg(PP_3)X_3$ (**9**−**10**) and $PtAg(PP_3)X_3$ (**11**−**12**).

$PdAg(PP_3)X_3$. The spectra of **9** and **10** consist of two signals. Assuming that the broad upfield resonance includes the phosphorus atoms P^B mutually trans bound to Pd(II) and P^C bound to Ag(I), their spectra at room temperature (Supporting Information, Figure S1) are compatible with the monomeric structure **I** shown in Scheme 1. Indeed, when the spectrum of **9** was recorded at 203 K (Figure 1) there appeared three intense broad resonances attributable to

(20) (a) Montes, J. A.; Rodríguez, S.; Fernández, D.; García-Seijo, M. I.; Gould, R. O.; García-Fernández, M. E. *J. Chem. Soc., Dalton Trans.* **2002**, 1110. (b) Attar, S.; Alcock, N. W.; Bowmaker, G. A.; Frye, J. S.; Bearden, W. H.; Nelson, J. H. *Inorg. Chem.* **1991**, *30*, 4166.

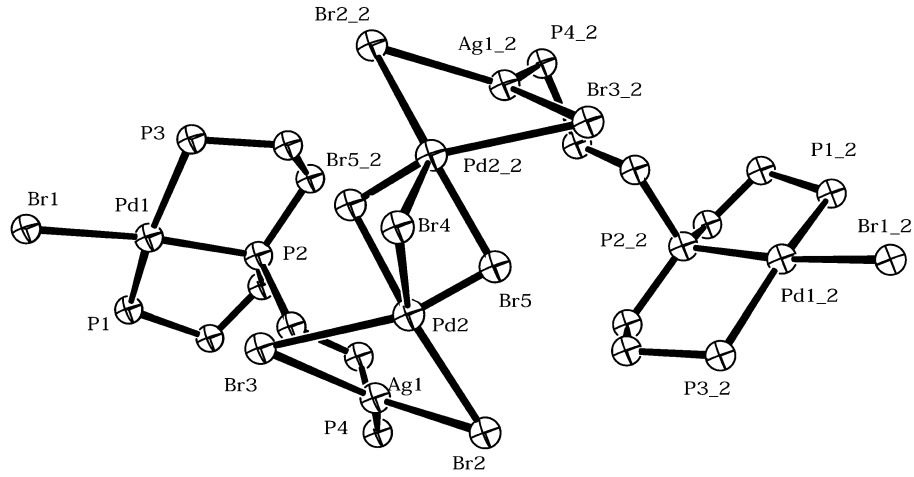

Figure 4. Ball-and-stick diagram for **10a**. Bromide counteranion and phenyl rings omitted for clarity.

Table 3. Summary of Crystal Parameters, Data Collection, and Refinement for **9**, **13**, **10a**, and **11a**

complex	**9**·CH_3OH·$2H_2O$	**13**	**10a**	**11a**·$CHCl_3$·H_2O
empirical formula	$C_{43}H_{42}P_4AgCl_3O_3Pd$	$C_{42}H_{42}P_4AgN_3O_9Pd$	$C_{42}H_{42}P_4AgBr_5Pd_2$	$C_{85}H_{84}P_8Ag_2Cl_9OPt_2$
formula weight	1051.35	1070.94	1390.86	2294.25
temperature (K)	293(2)	293(2)	293(2)	293(2)
wavelength (Å)	0.71073	0.71073	0.71073	0.71073
crystal size (mm)	0.54 × 0.40 × 0.08	0.32 × 0.16 × 0.12	0.40 × 0.22 × 0.09	0.50 × 0.40 × 0.35
color/habit	colorless/plates	colorless/prisms	colorless/prisms	colorless/prisms
crystal system	monoclinic	triclinic	monoclinic	triclinic
space group	*P*21	$P\bar{1}$	*C*2/*c*	$P\bar{1}$
a (Å)	13.3435(16)	10.616(7)	26.348(8)	16.144(5)
b (Å)	13.1677(17)	14.237(3)	9.770(3)	18.459(6)
c (Å)	14.3186(16)	16.691(3)	35.539(11)	18.548(6)
α (°)	90	70.330(15)	90	65.977(5)
β (°)	99.742(8)	82.04(4)	95.638(5)	81.592(5)
γ (°)	90	74.68(3)	90	77.054(5)
volume ($Å^3$)	2479.5(5)	2287.5(16)	9105(5)	4911(3)
Z	2	2	8	2
calculated density (Mg/m^3)	1.371	1.555	2.029	1.552
absorption coefficient (mm^{-1})	1.078	1.016	5.767	3.648
F(000)	1028	1080	5344	2250
θ range for data collection (°)	3.46 to 26.81	8.79 to 13.65	1.15 to 26.42	1.30 to 26.49
index ranges	$-18 \le h \le 13$	$-14 \le h \le 14$	$-32 \le h \le 32$	$-20 \le h \le 20$
	$-14 \le k \le 18$	$-17 \le k \le 19$	$0 \le k \le 12$	$-23 \le k \le 23$
	$-20 \le l \le 20$	$0 \le l \le 22$	$0 \le l \le 44$	$-23 \le l \le 23$
reflections collected	18312	11863	9883	54280
independent reflections	10188 [$R_{int} = 0.0717$]	11481 [$R_{int} = 0.0712$]	9322 [$R_{int} = 0.0872$]	20002 [$R_{int} = 0.0540$]
max. and min. transmission	1.000 and 0.725	0.978 and 0.767	0.6249 and 0.2063	0.3617 and 0.2628
data/restraints/parameters	10188/1/311	11481/0/541	9322/0/488	20002/0/964
goodness of fit on F^2	0.913	0.975	1.060	1.126
final R indices	$R_1 = 0.0749$	$R_1 = 0.0619$	$R_1 = 0.0840$	$R_1 = 0.0619$
	$wR_2 = 0.2081$	$wR_2 = 0.1501$	$wR_2 = 0.2599$	$wR_2 = 0.1994$
largest diff.peak and hole($eÅ^{-3}$)	1.483 and −1.390	1.187 and −1.174	1.871 and −4.158	3.159 and −1.483

phosphorus P^A, P^B, and P^C of monomer **I**. However, the averaged coupling constant P−Ag of 400 Hz obtained from the signal at *δ* 2.1 confirms the presence of Ag(I) bound to two P atoms (P^H in Scheme 1). This datum together with the broadening of the signals and the incipient appearance of two resonances at *δ* 93.0 and 72.0, characteristic of Pd(II) adopting a distorted square-planar P_2PdCl_2 geometry[17b] with $P_{central}$ and $P_{terminal}$ trans to Cl, respectively (P^F and P^G in Scheme 1), suggests the coexistence to some extent of the monomer **III** with the monomer **I**. Single crystals of the monomer **I** were studied (vide infra) by X-ray diffraction.

The heterohexanuclear fragment found for **10** in its mass spectrum seems to suggest that the distorted square-planar P_3PdBr and trigonal planar $PAgBr_2$ predicted arrangements to the metals correspond to an oligonuclear species with a 4:2 palladium to silver ratio. This is consistent with the presence of bromide bridges between both Ag(I)/Pd(II) and Pd(II)/Pd(II) centers as proposed for **10a** in Scheme 2. Thus, complex **10** undergoes oligomerization in solution to give **10a** (eq 1).

$$\underset{\mathbf{10}}{4PdAg(PP_3)Br_3} \xrightarrow[-2Ag(PP_3)Br]{DMSO\text{-}d_6} \underset{\mathbf{10a}}{[Pd_4Ag_2(PP_3)_2Br_9]Br} \quad (1)$$

Crystals of **10a**, afforded by the interaction between **4** and the excess AgBr, were studied by X-ray diffraction (vide infra).

$PtAg(PP_3)X_3$. The spectrum of **11** at room temperature (Supporting Information, Figure S2, Table 2) consists of three doublets and an incipient broad signal at *δ* 32.0. The coupling

Table 4. Selected Distances (Å) and Angles (deg.) for Complexes **9** and **13**

complex	**9**·CH_3OH·$2H_2O$	**13**
Pd(1)−P(1)	2.336(4)	2.334(2)
Pd(1)−P(2)	2.208(3)	2.202(2)
Pd(1)−P(3)	2.325(4)	2.296(2)
Ag(1)−P(4)	2.392(4)	2.361(3)
Pd(1)−Cl(1)	2.361(3)	
Pd(1)−O(11)		2.138(5)
N(1)−O(11)		1.281(8)
N(1)−O(12)		1.228(8)
N(1)−O(13)		1.226(8)
N(2)−O(21)		1.224(9)
N(2)−O(22)		1.269(9)
N(2)−O(23)		1.220(9)
N(3)−O(31)		1.134(1)
N(3)−O(32)		1.222(1)
N(3)−O(33)		1.254(2)
Ag(1)−Cl(2)	2.601(4)	
Ag(1)−Cl(3)	2.400(5)	
Ag(1)−O(21)		2.427(7)
Ag(1)−O(22)		2.430(7)
Ag(1)−O(31)		2.430(9)
P(1)−Pd(1)−P(2)	83.20(1)	84.71(8)
P(1)−Pd(1)−P(3)	162.85(1)	162.23(8)
P(2)−Pd(1)−P(3)	83.64(1)	84.62(8)
P(1)−Pd(1)−Cl(1)	98.82(1)	
P(2)−Pd(1)−Cl(1)	175.02(2)	
P(3)−Pd(1)−Cl(1)	95.19(2)	
P(1)−Pd(1)−O(11)		98.91(2)
P(2)−Pd(1)−O(11)		175.35(2)
P(3)−Pd(1)−O(11)		91.15(2)
P(4)−Ag(1)−Cl(2)	106.01(2)	
P(4)−Ag(1)−Cl(3)	145.57(2)	
P(4)−Ag(1)−O(21)		141.30(2)
P(4)−Ag(1)−O(22)		143.86(2)
P(4)−Ag(1)−O(31)		119.0(2)
Cl(2)−Ag(1)−Cl(3)	107.94(2)	
O(21)−Ag(1)−O(22)		52.4(2)
O(21)−Ag(1)−O(31)		93.6(4)
O(22)−Ag(1)−O(31)		83.8(3)

constants $^1J(^{31}P, ^{195}Pt)$ of 2898/2495 Hz obtained from the resonances at δ 90.1/44.4 are characteristic of a central phosphorus trans to Cl and a terminal phosphorus mutually trans, respectively, as in monomer **I**, while the coupling constant of 3590 Hz obtained from the signal at δ 11.0 is attributed to one terminal phosphorus trans to Cl, as in monomer **III**. The broad signal at δ 32.0 seems to include the phosphorus bound to silver. When the spectrum of **11** was recorded at 203 K the downfield signal shifts to δ 88.0, the one at δ 44.4 splits into two close resonances, and those at δ 32.0 and 11.0 shift to higher and lower field, giving broad peaks assigned to phosphorus bound to Ag(I) (P^C, P^H) and Pt(II) (P^F, P^G), respectively. The result was the spectrum shown in Figure 2. The $^1J(^{31}P, ^{195}Pt)$ coupling constants of 2948, 2494−2484, and 3687 Hz attributable to P^A trans to Cl, P^B mutually trans, and P^G trans to Cl, respectively, are in accordance with the coexistence of two oligomers, one afforded by combination of the monomers **I** + **III** and the other one the dimer **11a** shown in Scheme 2. The $^{195}Pt\{^1H\}$NMR spectrum at ambient temperature (Supporting Information, Figure S3) shows an overlapped doublet of doublets at δ −4420 with $^1J(^{31}P, ^{195}Pt)$ = 3642 Hz and an overlapped doublet of triplets at δ −4818 with $^1J(^{31}P, ^{195}Pt)$ = 2944 and 2471 Hz, consistent with the two types of environments to platinum observed in monomer **I**/oligomer **11a** and in monomer **III**. We afforded single crystals of the dimer **11a** that were studied by X-ray diffraction (vide infra).

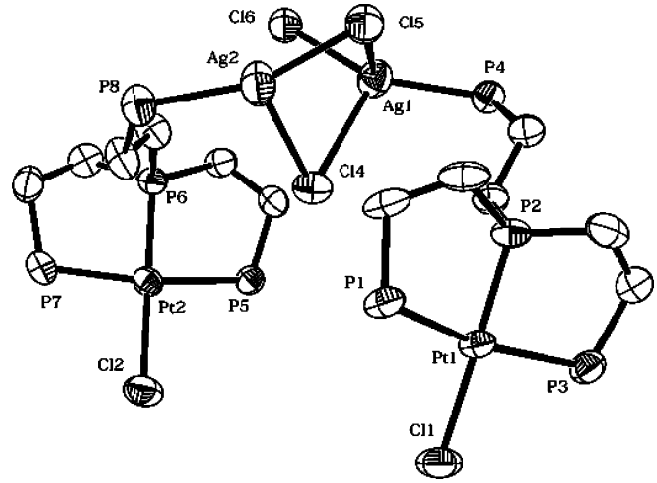

Figure 5. ORTEP diagram for **11a**. Chloride counteranion and phenyl rings omitted for clarity.

Complexes Containing Nitrates As Coligands. Complexes $MAg(PP_3)(NO_3)_3$ [M = Pd(**13**), Pt(**14**)] behave as conductors in dimethylformamide (DMF) solutions with conductivities in the higher limit for 2:1 electrolytes, which is consistent with substitutions of nitrate ions by solvent molecules as previously observed in other silver(I) nitrate derivatives containing polyphosphines.[21] The peaks at *m*/*e* 1009 (**13**) and 1098 (**14**) correspond to $MAg(PP_3)(NO_3)_2$ fragments in agreement with the formation of heteronuclear systems. The splitting of the bands assigned to ν_a(N−O) in the infrared spectra suggests the presence of mono- and bidentate nitrate.

The $^{31}P\{^1H\}$NMR spectra (Table 2) show three signals in a 1:2:1 integration ratio (Figure 2, **14**) assigned to phosphorus atoms P^A, P^B, and P^C, respectively, of the monomeric structure shown in Scheme 3. The $^1J(^{31}P, ^{195}Pt)$ couplings from the signals at lower field for **14** (3146/2616 Hz) confirm the presence of distorted square-planar Pt(II) with P^A trans to one oxygen atom of NO_3^- and P^B trans to P^B. The $^{195}Pt\{^1H\}$ NMR spectrum consists, as expected, of an overlapped doublet of triplets centered at δ −4680 (Supporting Information, Figure S3) that exhibits coupling constants, $^1J(^{31}P, ^{195}Pt)$, of 3096/2633 Hz in agreement with the proposed structure. Thus, $AgNO_3$ is able to induce the opening of one of the three chelate rings to M leading to a neutral complex with the unexpected presence of nitrate acting as both mono and bidentate ligand to Ag(I) as confirmed in the solid state by X-ray diffraction (vide infra). There is no ring-opening by adding excess $AgNO_3$ to **13** or **14** giving an explanation to the chloro substitution reactions undergone by [M(tripho-s)Cl]Cl compounds (with analogous distorted square-planar geometry to M) upon interaction with $AgNO_3$ (Scheme 3).

(21) Sevillano, P.; García, M. E.; Habtemariam, A.; Parsons, S.; Sadler, P. J. *Met.-Based Drugs* **1999**, *6*, 211.
(22) (a) Teo, B.-K.; Calabrese, J. C. *Inorg. Chem.* **1976**, *15*, 2467. (b) Bowmaker, G. A.; Hanna, J. V.; Healy, P. C.; Skelton, B. W.; White, A. H. *J. Chem. Soc., Dalton Trans.* **1993**, 1387. (c) Cassell, A. *Acta Crystallogr., Sect. B.* **1979**, 174. (d) Stein, R. A.; Knobler, C. *Inorg. Chem.* **1977**, *16*, 242. (e) Harper, C. S. W.; Tiekink, E. R. T. *Acta Crystallogr.* **1989**, *C45*, 1815.

Table 5. Selected Distances (Å) and Angles (deg.) for Complex **10a**

complex	**10a**
Pd(1)−P(1)	2.324(3)
Pd(1)−P(2)	2.215(3)
Pd(1)−P(3)	2.313(3)
Ag(1)−P(4)	2.385(4)
Pd(1)−Br(1)	2.460(2)
Ag(1)−Br(2)	2.615(2)
Ag(1)−Br(3)	2.619(2)
Ag(1)−Pd(2)	2.707(3)
Pd(2)-Pd(2_2)	2.823(6)
Pd(2)−Br(2)	2.538(4)
Pd(2)−Br(3)	2.796(4)
Pd(2)−Br(4)	2.573(3)
Pd(2)−Br(5)	1.725(6)
Pd(2_2)-Br(5)	2.250(6)
Br(4)−Br(5)	2.762(6)
P(1)−Pd(1)−P(2)	84.18(1)
P(1)−Pd(1)−P(3)	157.47(1)
P(2)−Pd(1)−P(3)	84.14(1)
P(1)−Pd(1)−Br(1)	97.57(9)
P(2)−Pd(1)−Br(1)	171.57(1)
P(3)−Pt(1)−Br(1)	96.81(1)
P(4)−Ag(1)−Br(2)	121.62(1)
P(4)−Ag(1)−Br(3)	128.38(1)
Br(2)−Ag(1)−Br(3)	108.60(1)
Ag(1)−Br(2)−Pd(2)	63.37(9)
Ag(1)−Br(3)−Pd(2)	59.89(8)
Pd(2)−Br(5)−Pd(2_2)	89.5(3)
Br(2)−Pd(2)−Br(4)	132.32(2)
Br(2)−Pd(2)−Br(5_2)	155.5(2)
Br(2)−Pd(2)−Br(3)	105.53(1)
Br(2)−Pd(2)−Br(5)	86.4(2)
Br(3)−Pd(2)−Br(4)	106.06(1)
Br(3)−Pd(2)−Br(5)	157.9(3)
Br(3)−Pd(2)−Br(5_2)	72.34(2)
Br(4)−Pd(2)−Br(5)	77.2(2)
Br(4)−Pd(2)−Br(5−2)	69.50(2)
Br(5)−Pd(2)−Br(5_2)	89.0(3)
Br(5)−Br(4)−Br(5_2)	61.2(2)

Table 6. Selected Distances (Å) and Angles (deg.) for Complex **11a**

complex	**11a**·$CHCl_3$·H_2O
Pt(1)−P(1)	2.318(3)
Pt(1)−P(2)	2.213(3)
Pt(1)−P(3)	2.317(3)
Pt(2)−P(5)	2.317(3)
Pt(2)−P(6)	2.226(3)
Pt(2)−P(7)	2.314(3)
Ag(1)−P(4)	2.395(3)
Ag(2)−P(8)	2.382(4)
Pt(1)−Cl(1)	2.361(3)
Pt(2)−Cl(2)	2.390(3)
Ag(1)−Cl(4)	2.746(3)
Ag(1)−Cl(5)	2.872(4)
Ag(1)−Cl(6)	2.464(4)
Ag(2)−Cl(4)	2.664(3)
Ag(2)−Cl(5)	2.420(4)
P(1)−Pt(1)−P(2)	85.12(1)
P(1)−Pt(1)−P(3)	161.32(1)
P(2)−Pt(1)−P(3)	84.44(1)
P(5)−Pt(2)−P(6)	84.59(1)
P(5)−Pt(2)−P(7)	159.54(1)
P(6)−Pt(2)−P(7)	84.44(1)
P(1)−Pt(1)−Cl(1)	97.08(1)
P(2)−Pt(1)−Cl(1)	175.06(1)
P(3)−Pt(1)−Cl(1)	94.58(1)
P(5)−Pt(2)−Cl(2)	96.47(1)
P(6)−Pt(2)−Cl(2)	174.58(1)
P(7)−Pt(2)−Cl(2)	96.08(1)
P(4)−Ag(1)−Cl(4)	110.08(1)
P(4)−Ag(1)−Cl(5)	100.00(1)
P(4)−Ag(1)−Cl(6)	144.70(1)
P(8)−Ag(2)−Cl(4)	105.34(1)
P(8)−Ag(2)−Cl(5)	157.30(1)
Cl(4)−Ag(1)−Cl(5)	85.55(1)
Cl(4)−Ag(1)−Cl(6)	99.99(1)
Cl(5)−Ag(1)−Cl(6)	100.35(1)
Cl(4)−Ag(2)−Cl(5)	97.18(1)
Ag(1)−Cl(4)−Ag(2)	73.08(9)
Ag(1)−Cl(5)−Ag(2)	74.45(9)

The analogous reaction, with 3 equiv of $AgNO_3$, for complex **1** was also followed by $^{31}P\{^1H\}$NMR, and a mixture of the heterobimetallic complex $PdAg(NP_3)Cl_2(NO_3)$ and $[Pd(NP_3)(ONO_2)](NO_3)$ seems to be formed. However, there was no reaction between $AgNO_3$ and $[Pt(NP_3)X]X$ (X = Cl, Br)[18] in agreement with the higher inertness of Pt(II) compared to Pd(II).

Crystallography of 9·CH_3OH·$2H_2O$, 10a, 11a·$CHCl_3$·H_2O, and 13. Oak Ridge Thermal Ellipsoid Plot (ORTEP) diagrams are shown in Figures 3 and 5, and Figure 4 shows a ball-and-stick diagram for **10a**. Summaries of crystal parameters, data collection, and refinement are given in Table 3, and selected bond lengths and angles are listed in Tables 4–6. The unit cell for **9/13** and **11a** consists of two neutral $PdAg(PP_3)X_3$ (X = Cl, NO_3) molecules and cation−anion $[Pt_2Ag_2(PP_3)_2Cl_5]^+Cl^-$ pairs, respectively, while for **10a** it consists of eight cation−anion $[Pd_4Ag_2(PP_3)_2Br_9]^+Br^-$ pairs stacked as shown in Supporting Information, Figure S4. The complexes exhibit a distorted square-planar geometry to Pd(1) or Pt(1)/Pt(2) bound to three P atoms and one monodentate anionic ligand with silver being bound to one dangling phosphorus of PP_3. Silver(I) completes the three-coordination in **9** and **10a** with two halides and the four-coordination in **13** with two nitrates, one acting as monodentate and the other one as bidentate ligand. In complex **11a** the two square-planar $ClPtP_3P$ fragments, containing a dangling phosphorus, are bridged via disilver, $Ag(\mu\text{-}Cl)_2Ag$, units where the metals afford trigonal planar, $PAgCl_2$, and tetrahedral, $PAgCl_3$, environments. Complex **10a** contains two $BrPdP_3PAgBr_2$ fragments with distorted square-planar and trigonal planar Pd(II) and Ag(I) centers, respectively, that are connected via bromide bridges by an unusual $Pd(\mu\text{-}Br)_3Pd$ unit showing distorted trigonal bipyramidal $PdBr_5$ arrangements. The Ag−P bond distances [2.392(4), 2.361(3), 2.385(4) and 2.395(3)−2.382(4) Å for **9**, **13**, **10a**, and **11a**, respectively] are within the values found for $Ag_2(CP_3)Cl_2$[20a] (CP_3 = 1,1,1-tris(diphenylphosphinomethyl)ethane) (2.364−2.463 Å), consisting of infinite chains with three- ($PAgCl_2$) and four-coordinate (P_2AgCl_2) silver geometries, lie at the short end of the range observed for silver(I) complexes containing PPh_3 such as $[Ph_3PAgCl]_4$ (av. 2.382 Å),[22a] $[(Ph_3P)_2AgX]_2$ [av. 2.476 Å (X = Cl), 2.496 Å (X = Br)],[22b,c] Ph_3PAgNO_3 (2.369 Å),[22d] or $(Ph_3P)_2AgNO_3$ (2.434 Å)[22e] and are measurably shorter than those observed for $Ag(NP_3)Cl$ (2.516−2.549 Å) where silver shows a distorted tetrahedral AgP_3Cl arrangement.[20a] As expected,[23] the Ag−P bond lengths for **9**, **10a**, **11a**, and **13** are longer than the Au−P distances (2.310 Å) found for $[PtAu(PP_3)X_2]X$ (X = Cl, Br).[17b]

The MP_3X environments [M = Pd, X = Cl (**9**), Br (**10a**), NO_3 (**13**); M = Pt, X = Cl (**11a**)] determine two fused five-

(23) Bachman, R. E.; Andretta, D. F. *Inorg. Chem.* **1998**, *37*, 5657.

membered rings to M as was observed for [Pd(triphos)Cl]Cl,[2] [Pd(triphos)(ONO_2)](NO_3),[16] or [Pt(triphos)Cl]Cl.[1h] The M−$P_{central}$ bond distances [2.208(3), 2.202(2), 2.215(3), and 2.213(3)−2.226(3) Å for **9**, **13**, **10a**, and **11a**, respectively) are shorter than the M−$P_{terminal}$ because of the double chelate effect, and both are in the expected range.[24] As previously observed, the weaker and stronger trans influence of the Pd(1)−O and Pd(1)−Br bonds, respectively, compared to Pd−Cl[16,25] leads to Pd−$P_{central}$ distances for **13** and **10a** that are shorter and longer, respectively, than for **9**. All M−X distances [2.361(3) (Pd−Cl), 2.138(5) (Pd−O), 2.460(2) (Pd(1)−Br) and 2.361(3)−2.390(3) Å (Pt−Cl) for **9**, **13**, **10a**, and **11a**, respectively] are longer than those found in the analogous complexes [M(triphos)X]X[16,1h,25] or [PtAu(PP_3)Cl_2]Cl[17b] and are very close to the values found for other square-planar M(II) phosphino compounds containing two M−X bonds (X = Cl, Br).[1h,17b] However, the M−Cl bond lengths for **9** and **11a** are shorter than the axial M−Cl distances for the trigonal-bipyramidal precursors **3** (2.418 Å)[26] and **5** (2.420 Å),[19] respectively, as also predicted by far-infrared spectra. On the other hand, Ag−Cl distances [2.601(4), 2.400(5) Å (**9**), and 2.464(4), 2.746(3)−2.872(4), 2.420(4)−2.664(3) Å (**11a**)] are longer than Pd−Cl (**9**) or Pt−Cl (**11a**) which is in agreement with ν(Ag−Cl) being at lower wavenumber than ν(M−Cl). Again, because the atomic radii of gold atoms are smaller than those of silver atoms the terminal Ag−Cl bond length in **11a** is longer than the corresponding Au−Cl bond distance in [PtAu(PP_3)Cl_2]Cl. It should be noted that, as previously found for other silver(I) complexes with phosphines and Ag_2Cl_2 bridging units, one chloride is more strongly bound to the silver center giving a shorter Ag−Cl distance. For **11a**, Cl(5) is involved in both the shortest [2.420(4) Å, Ag(2)−Cl(5)] and the longest [2.872(4) Å, Ag(1)−Cl(5)] Ag−Cl bond lengths with the averaged Ag−Cl bridging distance of 2.676(4) Å being significantly greater than the analogous distance, established by theoretical studies, for [ClAgPH_3]$_2$ of 2.450 Å.[15c]

Complex **10a** exhibits Ag(1)−Pd(2), Pd(2)−Pd(2_2) and Br(4)−Br(5) contacts of 2.707(3), 2.823(6), and 2.762(6) Å, respectively, and, as was observed for **11a**, one of the bromine atoms of the Ag(1)(μ-Br)$_2$Pd(2) and Pd(2)(μ-Br)$_3$Pd(2_2) units is more strongly bound to one metal center [2.615(2)/2.619(2) Å for Ag(1) bound to Br(2)/Br(3), 2.538(4)/2.796(4)/2.573(3)/1.725(6) Å for Pd(2) bound to Br(2)/Br(3)/Br(4)/ Br(5), respectively, and 2.250(6) Å for Pd(2_2)−Br(5)].

The N−O bond distance corresponding to the oxygen bound to Pd(II) for **13** (1.281(8)Å) is longer than the analogous distance found in [Pd(triphos)(ONO_2)](NO_3)[16] (1.265(5) Å) and both are longer than the two N−O distances of the anion involving uncoordinated oxygens [1.228(8) and 1.226(8) Å] which can be interpreted as a consequence of the decrease in the N−O bond order. The Ag−O bond lengths for the bidentate (2.427(7) and 2.430(7) Å) and monodentate (2.430(9) Å) nitrates are shorter than those found in other compounds containing tetrahedral silver(I) as [Ag(P(C_6H_4Me)$_3$)$_2$(O_2NO)] (2.516 Å)[27] and [Ag_2(dppm)$_2$(O_2NO)$_2$] (2.689 Å).[28] Once again, the N−O bond distances involving coordinated oxygen atoms [1.244(9), 1.269(9) Å] of the bidentate NO_3^- are longer than the N−O bond length because of the uncoordinated one [1.220(9) Å]. However, the chelate effect of the bidentate anion leads to a N−O distance corresponding to the coordinated oxygen atom of the monodentate nitrate [1.134(1) Å] shorter than those due to the uncoordinated ones [1.222(1) and 1.254(2) Å].

The palladium, Pd(1), or platinum, Pt(1), atom is displaced 0.057 Å (**9**), 0.1681 Å (**13**), 0.0995 (**10a**), and 0.1038 Å (**11a**) from the least-squares plane defined by [P(1), P(2), P(3), X], and Pt(2) is displaced −0.1122 Å from the plane [P(5),P(6),P(7),Cl(2)]. Their coordination sphere is tetrahedrally distorted from planar arrangement with the two mutually trans phosphorus atoms on one side and the donor atom of X together with the phosphorus atom trans to X on the opposite side.

The P−M−P and P−M−X angles of 162.85−83.42av.° (**9**); 162.23−84.67av.° (**13**); 157.47−84.16av.° (**10a**); 160.4−84.7av.° (**11a**); and 175.0−97.0av.° (**9**); 175.35−95.03av.° (**13**); 171.57−97.20av.° (**10a**); 174.8−96.1av.° (**11a**), respectively, confirm the distorted square-planar geometry to Pd(1) or Pt(1)/Pt(2).

The monodentate nitrates bound to the metals in **13** retain the trigonal-planar geometry although slightly distorted because of the coordination effect, showing O−N−O angles of 124.7, 118.5, and 116.7° for NO_3^- bound to Pd(II) and 128.6, 122.6, and 108.8° for the nitrate bound to Ag(I).

The three-coordinate units $PAgCl_2$ in **9**, **10a**, and **11a** are almost planar with Ag(1) deviating from the planes by 0.091 Å, 0.1721 Å, and 0.0357 Å, respectively, and with the sum of angles around the metal atom not differing much from 360° [359.5° (**9**), 358.6 (**10a**), and 359.8 (**11a**)]. The $PAgCl_3$ unit of **11a** exhibits P−Ag−Cl [av. 105.1, 151.0°] and Cl−Ag−Cl (av. 95.8°) angles which differ from the expected for the ideal tetrahedral geometry demonstrating the distortion. For **10a** Pd(2) is displaced 0.1897 Å from the plane Br(2), Br(4), Br(5_2), and the angles Br(2)−Pd(2)−Br(4) (132.32(15)°), Br(3)−Pd(2)−Br(5) (157.9(3)°), and Br(3)−Pd(2)−Br(4) (106.06(11)°) make evident the distortion from the ideal trigonal bipyramidal geometry.

Finally, **10a** and **11a** show metallophilic contacts [Pd(2)−Pd(2_2) and Ag(1)−Pd(2) of 2.823(6) and 2.707(3) Å, respectively, for **10a** and Ag(1)−Ag(2) of 3.222 Å for **11a**] that in case of **11a** are stronger than those found in $Ag_2(CP_3)Cl_2$ (3.385 Å)[20] and weaker than those found in [Ag(PPh_3)I]$_4$ (3.095 Å)[29] and [Ag(py)(PPh_3)I]$_2$ (2.956 Å).[30,31] While preliminary studies on luminescence for $Ag_2(CP_3)Cl_2$

(24) Orpen, A. G.; Brammer, L.; Allen, F. H.; Kennard, O.; Watson, D. G.; Taylor, R. *J. Chem. Soc., Dalton Trans.* **1989**, S1.
(25) Housecroft, C. E.; Shaykh, B. A. M.; Rheingold, A. C. *Acta Crystallogr., Sect. C* **1990**, *46*, 1549.
(26) Aizawa, S.; Iida, T.; Funahashi, S. *Inorg. Chem.* **1996**, *35*, 5163.
(27) Liu, C. W.; Pau, H.; Fackler, J. P., Jr.; Wu, G.; Wasylishen, R. E.; Shang, M. *J. Chem. Soc., Dalton Trans.* **1995**, 3691.
(28) Ho, D. M.; Bau, R. *Inorg. Chem.* **1983**, *22*, 4073.
(29) Teo, B. K.; Calabrese, J. C. *Inorg. Chem.* **1976**, *15*, 2474.
(30) Gotsis, S.; Engelhardt, L. M.; Healy, P. C.; Kilden, J. D.; White, A. H. *Aust. J. Chem.* **1989**, *42*, 923.
(31) Engelhardt, L. M.; Healy, P. C.; Skelton, W.; White, A. H. *Aust. J. Chem.* **1991**, *44*, 1585.

point to an emissive behavior in the solid state, complex **11a** showing argentophilicity does not luminesce in the solid state neither at 298 nor 77 K. There are no unusual interactions between the cation and the bromide and chloride anions of **10a** and **11a** which are located close to the $Ag(\mu\text{-}Br)_2Pd$ bridges and the square-planar $PtPP_2Cl$ unit containing Pt(1), respectively.

Silver(I) and Gold(I) As Inductors of Ring-Opening Reactions. The use of silver(I) halides as inductors of ring-opening processes introduces a complexity in the number of isomers/oligomers formed that was not found for gold(I), and the use of $AgNO_3$ allowed us to characterize, by X-ray diffraction, the first structure of a monomeric heterobimetallic compound containing $Pd-ONO_2$ and $O_2NO-Ag-O_2NO$ bonds. The nitrate coordination to palladium(II) in crystallographically characterized compounds is not very common,[16] and to the best of our knowledge, the achievement of an adduct bearing monodentate and bidentate nitrates to the same silver(I) center is unprecedented.

The number of the generated ring-openings varies with the polyphosphine ligand and the inductor. Thus, while the reaction of **1** and **2** with Au(I) occurs via a single ring-opening process and the double ring-opening afforded by interaction with silver(I) halides is not predominant, Au(I) induces a single and double chelate ring-opening of **3** and **5** by reaction with one and two equivalents of Au(tdg)Cl,[17b] respectively, and the prevailing single ring-opening reaction of **3** and **5** with AgX is not dependent on the stoichiometric ratio (vide supra).

The smaller size of gold atoms compared to silver atoms that leads to a preference for coordination number two over three for gold in contrast to silver contributes to explain the different extent of these ring-openings. The size of the metal, M, and the halide, X, also seem to play a role in the nuclearity of the systems resulting for M = Pd and X = Br in the best combination that affords the unexpected complex **10a** containing two five-coordinate palladium(II) centers ($PdBr_5$) together with one Pd···Pd and two Ag···Pd contacts. On the other hand, the similarities between **10a** and **11a** with six and four metal atoms, respectively, are evident. Both are rare examples of heterobimetallic oligomers where one of the metals of the halide bridging units involving Pd(II)/Ag(I) or Ag(I)/Ag(I) achieves a coordination number (five for Pd(II) in **10a** and four for Ag(I) in **11a**) above the usual, resulting in unexpected large monocationic complexes with just one halide as counteranion. However, complex **9** was prepared as a monomeric neutral compound, and the counterpart MAu complexes with PP_3, corresponding to the first ring-opening of the precursors, were monomeric ionic species. The analogous MCu systems afforded by addition of one and two equivalents of CuCl[17a] to the precursors were characterized as neutral and monomeric ionic compounds, respectively. This tunable nuclearity and ionicity of the PdM′ and PtM′ (M′ = Cu, Ag, Au) systems could provide a valuable method in the design of heteronuclear materials with desirable properties and applications.

Conclusions

The five coordinate complexes $[Pd(NP_3)X]X$ and $[M(PP_3)X]X$ (X = Cl, Br; M = Pd, Pt) react with AgX salts (X = Cl, Br, NO_3) to give new heteronuclear compounds via a ring-opening process unexpectedly induced by silver(I). The nuclearity and ionicity of compounds afforded by interaction between AgX and $[M(PP_3)X]X$ (X = Cl, Br) was dependent on the metal M and for M = Pd on the halide anion. Crystallographic studies for chlorides reveal a neutral monomeric, $PdAg(PP_3)Cl_3$, and ionic dimeric, $[Pt_2Ag_2(PP_3)_2Cl_5]Cl$, structure with distorted square-planar palladium(II) and platinum(II) centers and with silver(I) showing trigonal-planar and both trigonal planar and tetrahedral geometries, respectively. $PdAg(PP_3)Br_3$ oligomerizes in solution to give $[Pd_4Ag_2(PP_3)_2Br_9]Br$ (also prepared by addition of excess AgBr to $[Pd(PP_3)Br]Br$) with the crystal structure showing that the cation contains two distorted square-planar palladium(II) centers connected via bromide bridges involving trigonal planar ($PAgBr_2$) and distorted trigonal bipyramidal ($PdBr_5$) units. Despite the weakly coordinating behavior of the nitrate anions, the reaction between excess $AgNO_3$ and $[M(PP_3)Cl]Cl$ takes place with formation of neutral monomeric species of the type $MAg(PP_3)(NO_3)_3$ containing M−O and Ag−O bonds with distorted square-planar and tetrahedral geometries to M(II) and Ag(I), respectively. The new compounds are rare examples of bimetallic species bearing nitrates acting as both mono and bidentate ligands to Ag(I). However, there is no ring-opening process induced by Ag(I) when excess $AgNO_3$ interacts with [M(triphos)Cl]Cl giving $[M(triphos)(ONO_2)](NO_3)$. The ability of the new mixed metal complexes to undergo a variety of reactions will be presented in the near future.

Experimental Section

General Procedures. Palladium chloride, palladium bromide, and potassium tetrachloroplatinate were purchased from Strem Chemicals, silver chloride, silver bromide and tris[2-(diphenylphosphino)ethyl]phosphine from Aldrich, sodium chloride and bromide from Panreac. Microanalyses were performed on a Fisons Instrument EA 1108 CHNS-O. Fast Atom Bombardment (FAB) or Liquid Secondary-Ion (LSI MS) mass spectra were obtained in a Micromass Autospec spectrometer using nitrobenzylic alcohol as the matrix. Infrared spectra were recorded at ambient temperature as KBr pellets (4000−500 cm^{-1}) and Nujol mulls (500−100 cm^{-1}) on a Mattson Cygnus 100 spectrophotometer. The bands are reported as vs = very strong, s = strong, m = medium, w = weak, sh = shoulder, br = broad. $^{31}P\{^1H\}$ and $^{195}Pt\{^1H\}$ NMR spectra were recorded on a Bruker AMX500 spectrometer at 202.46 and 107.52 MHz, respectively. A 2 s relaxation delay and a 30 degree pulse angle were used to favor measurable integration data on the $^{31}P\{^1H\}$ spectra. Chemical shifts (δ) are reported in ppm relative to external 85% H_3PO_4 (^{31}P) and 1 M Na_2PtCl_6 (^{195}Pt); s = singlet, d = doublet, t = triplet, dd= doublet of doublets, dt = doublets of triplets, dq = doublet of quartets, br = broad signal, J = coupling constant in Hz. Conductivities were measured at 25 °C using 10^{-3} M solutions in DMF or CH_3CN on a WTW model LF-3 instrument.

Tris(2-diphenylphosphinoethyl)amine (NP_3) was prepared following the procedures previously described.[18,32]

Preparation of $PdAg(NP_3)X_3$ [X = Cl(7), Br (8)]. To a solution of $[Pd(NP_3)X]X\cdot 2H_2O$ (X = Cl, Br)[17b] (0.1569−0.1731 mmol) in MeOH (25 mL) was added AgX as solid in a 1:2 stoichiometric ratio, and the reaction mixtures were stirred for 14−22 h protected from the light. After that, excess of AgX (X = Cl, Br) was removed by filtration (when X = Br, the methanol was previously removed in vacuo from the suspension formed to give a solid, which was completely dissolved in CH_2Cl_2 leaving the unreacted silver salt). The solvent was partially removed in vacuo, and Et_2O was added to complete the precipitation. The solid was filtered off and dried in vacuo. **7**: Yield: 61%, bright yellow solid, mp 212 °C (dec.). Found: C, 51.5; H, 5.0; N, 1.5. $C_{42}H_{42}NP_3PdAgCl_3$ requires: C, 51.8; H, 4.3; N, 1.4%. **8**·Et_2O: Yield: 61%, greenish yellow solid, mp 203 °C (dec.). Found: C, 47.0; H, 5.1; N, 1.4. $C_{46}H_{52}NP_3PdAgBr_3O$ requires: C, 46.8; H, 4.5; N, 1.2%.

Preparation of $MAg(PP_3)X_3$ [M = Pd, X = Cl (9), Br (10); M = Pt, X = Cl (11), Br (12); M = Pd, X = NO_3 (13); M = Pt, X = NO_3 (14)]. To a solution of $[M(PP_3)X]X\cdot nH_2O$ (M = Pd, Pt; X = Cl, Br)[17b] (0.0733−0.1714 mmol) in $CHCl_3$ (25−50 mL) were added AgX as solid in 1:1 stoichiometric ratio or $AgNO_3$ in MeOH (15−20 mL) in 1:3 stoichiometric ratio, and the reaction mixtures were stirred for 8−48 h protected from the light (in the case of the nitrate derivatives the silver chloride precipitate, formed inmediately after addition, was removed by filtration). The mixture for obtaining complex **11** was refluxed for 6 h until the silver salt dissolved completely. Et_2O was added to the final solutions precipitating in all cases a solid which was filtered off and dried in vacuo. (**9**)·$2H_2O$: Yield: 85%, pink solid, mp 186 °C. Found: C, 49.3; H, 4.5. $C_{42}H_{46}P_4PdAgCl_3O_2$ requires: C, 49.1; H, 4.5%. (**10**)·$4H_2O$: Yield: 77%, pink solid, mp 190 °C. Found: C, 41.9; H, 4.0. $C_{42}H_{50}P_4PdAgBr_3O_4$ requires: C, 42.1; H, 4.2%. **11**: Yield: 97%, yellow solid, mp 175 °C. Found: C, 46.0; H, 4.0. $C_{42}H_{42}P_4PtAgCl_3$ requires: C, 46.7; H, 3.9%. (**12**)·$0.5Et_2O$: Yield: 69%, yellow solid, mp 220 °C. Found: C, 42.6; H, 4.4. $C_{44}H_{47}P_4PtAgBr_3O_{0.5}$ requires: C, 43.5; H, 4.3%. (**13**)·$2H_2O$·$0.5Et_2O$: Yield: 62%, beige solid, mp 178 °C. Found: C, 45.6; H, 4.6; N, 3.9. $C_{44}H_{51}P_4PdAgN_3O_{11.5}$ requires: C, 46.1; H, 4.6; N, 3.7%. (**14**)·$2H_2O$·Et_2O: Yield: 77%, beige solid, mp 260 °C. Found: C, 43.8; H, 4.7; N, 3.5. $C_{46}H_{56}P_4PtAgN_3O_{12}$ requires: C, 43.5; H, 4.4; N, 3.3%.

Preparation of Crystals. Solutions of (**9**)·$2H_2O$ and **11** (0.0125−0.0195 mmol) in CH_2Cl_2 and $CHCl_3$, respectively, (1−2 mL) were filtered and stored in a vial protected from the light at 25 °C. Single crystals of **9**·CH_3OH·$2H_2O$ and **11a**·$CHCl_3$·H_2O were afforded by a vapor diffusion technique (of methanol) and slow evaporation, respectively. Single crystals of **13/10a** were prepared by addition of three/two equivalents of $AgNO_3$ (in CD_3OD)/AgBr (as a solid) to solutions of the precursors (**3**)·$4H_2O$/(**4**)·$2H_2O$ in $CDCl_3$. The mixtures were stirred for 24 h protected from the light, and solids were removed by filtration. Crystals used for X-ray diffraction were afforded from the solutions by slow evaporation.

X-ray Crystallography. Colorless plates of **9**·CH_3OH·$2H_2O$ and colorless prisms of **13**, **10a**, and **11a**·$CHCl_3$·H_2O were mounted on glass fibers and used for data collection. Crystal data were collected at 293(2) K using a BRUKER SMART CCD 1000 diffractometer for complexes **9**·CH_3OH·$2H_2O$, **10a**, and **11a**·$CHCl_3$·H_2O and on an Enraf Nonius MACH3 automatic diffractometer[33] for complex **13**. Graphite monochromated Mo Kα radiation was used throughout. The data for complexes **9**·CH_3OH·$2H_2O$, **10a** and **11a**·$CHCl_3$·H_2O were processed with SAINT,[34] and empirical absorption correction was made using SADABS.[35] The data for complex **13** were corrected for Lorentz and polarization effects,[36] and a semiempirical absorption correction (psi-scans) was made.[37] The structures were solved by direct methods using the program SHELXS-97[38] and SIR-92[39] in the case of **10a**. All of them were refined by full-matrix least-squares techniques against F^2 using SHELXL-97.[40] Positional and anisotropic atomic displacement parameters were refined for all non-hydrogen atoms. Hydrogen atoms were placed geometrically, and positional parameters were refined using a riding model. Atomic scattering factors were obtained with the use of International Tables for X-ray Crystallography.[41] Molecular graphics were obtained from ORTEP-3 for Windows.[42] The large thermal ellipsoids found for bromides in **10a** were attributed to the low quality of the crystals.

Acknowledgment. We thank Xunta de Galicia (Spain) for financial support.

Supporting Information Available: Crystallographic information files for **9**, **10a**, **11,** and **13** (CIF); Figures S1 and S2 displaying the $^{31}P\{^1H\}$NMR spectra for **7** at 213K, (**9**)·$2H_2O$ and **11** at room temperature, Figure S3 exhibiting the $^{195}Pt\{^1H\}$ NMR spectra for **11** and **14**, and Figure S4 showing a view of the unit cell for **10a** (PDF). This material is available free of charge via the Internet at http://pubs.acs.org.

IC702419R

(32) (a) García-Seijo, M. I.; Habtemariam, A.; Murdoch, P. del S.; Gould, R. O.; García-Fernández, M. E. *Inorg. Chim. Acta* **2002**, *335*, 52. (b) García-Seijo, M. I.; Habtemariam, A.; Parsons, S.; Gould, R. O.; García-Fernández, M. E. *New J. Chem.* **2002**, *26*, 636.

(33) Nonius, B. V. *CAD4-Express Software*, Ver. 5.1/1.2; Enraf Nonius: Delft, The Netherlands, 1994.

(34) *SMART and SAINT, Area Detector Control and Integration Software*; Bruker Analytical X-ray Instruments Inc.: Madison, WI, 1997.

(35) Sheldrick, G. M. *SADABS, Program for Empirical Absorption Correction of Area Detector Data*; University of Goettingen: Goettingen, Germany, 1997.

(36) Kretschmar, M. *GENHKL Program for the reduction of CAD4 Diffractometer data*; University of Tuebingen: Germany, 1997.

(37) North, A. C. T.; Phillips, D. C.; Mathews, F. S. *Acta Crystallogr.* **1968**, *A24*, 351.

(38) Sheldrick, G. M. *Acta Crystallogr.* **1990**, *A46*, 467.

(39) Altomare, A.; Cascarano, G.; Giacovazzo, C.; Guagliardi, A. *J. Appl. Crystallogr.* **1993**, *26*, 343–350; SIR92, A program for crystal structure solution.

(40) Sheldrick, G. M. *SHELXL-97, Program for the Refinement of Crystal Structures*; University of Goettingen: Goettingen, Germany, 1997.

(41) *International Tables for X-ray Crystallography*; Kluwer Academic Publishers: Dordrecht, The Netherlands, 1995; Vol. C.

(42) Farrugia, L. J. *J. Appl. Crystallogr.* **1997**, *30*, 565.